Available online at www.sciencedirect.com
SCIENCE DIRECT®
International Journal of Pharmaceutics 290 (2005) 161–172
international journal of pharmaceutics
www.elsevier.com/locate/ijpharm

Pharmaceutical Nanotechnology

Loading efficiency of stavudine on polybutylcyanoacrylate and methylmethacrylate-sulfopropylmethacrylate copolymer nanoparticles

Yung-Chih Kuo*

Department of Chemical Engineering, National Chung Cheng University, Chia-Yi 62102, Taiwan, Republic of China

Received 1 October 2004; received in revised form 25 November 2004; accepted 27 November 2004

Abstract

Loading efficiency (LE) of stavudine (D4T), a human immunodeficiency antiretroviral agent, on the external surfaces of polybutylcyanoacrylate (PBCA) and methylmethacrylate-sulfopropylmethacrylate (MMA-SPM) was investigated. The experimental results indicate that the larger the polymeric nanoparticles (NPs), the smaller LE of D4T on the two kinds of biomaterials. Freeze drying of the two NPs, however, yields an increase in particle size and an increase in LE of D4T, in general. Preservation of the two D4T-loaded NPs through cold storage at 4 °C over 6 weeks leads to an increase in particle size and a decrease in LE of D4T. LE of D4T on both of the two NPs decreases with a variation in pH value from pH 7.2 of loading medium. LE of D4T on MMA-SPM NPs is larger than that on PBCA NPs at pH 7.4; and for the case of variation in pH value of loading medium from pH 7.2, the extent of decrease in LE of D4T for MMA-SPM NPs is higher than that on PBCA NPs. These outcomes imply that for oral administration, D4T-loaded MMA-SPM NPs may be more advantageous than D4T-loaded PBCA NPs, and D4T-loaded PBCA NPs may be more favorable than D4T-loaded MMA-SPM NPs for intravenous injection.

Keywords: Stavudine (D4T); Nanoparticle; Drug loading; Lyophilization; Cold storage

1. Introduction

The essential material characteristics of an ideal drug carrier include (1) biocompatibility and bioacceptability of the carrier and its degradation products, (2) ability to be loaded with effective dosage, (3) acceptable stability during preservation, (4) satisfactory drug-release rate from the drug-loaded composite, (5) suitable for regular clinical administration, and (6)

Abbreviations: D4T, stavudine; HIV, human immunodeficiency virus; LE, loading efficiency (%); MMA-SPM, methylmethacrylate-sulfopropylmethacrylate; NP, nanoparticle; NRTI, nucleoside reverse transcriptase inhibitor; PBCA, polybutylcyanoacrylate; PDI, polydispersity index; SPM, sulfopropylmethacrylate

* Tel.: +886 5 272 0411x33459; fax: +886 5 272 1206.
E-mail address: chmyck@ccu.edu.tw.

0378-5173/$ – see front matter © 2004 Elsevier B.V. All rights reserved.
doi:10.1016/j.ijpharm.2004.11.025

Nomenclature

D_{av}	average particle diameter (nm)
MW_{na}	number-averaged molecular weight (Da)
pH_m	medium pH value for the minimum D_{av}
t	synthesis time (h)
t_c	characteristic t for dramatic increase in D_{av} (h)
w	stirring rate (rpm)

economically feasible for manufacture. Since the average diameter of human microvessels is between 5 and 10 μm, a drug carrier with diameter less than 1 μm can be considered as a candidate for the application to intravenous injection. For drug delivery into the central nervous system, an increase in osmotic pressure can be aggressive and may bring other substances into brain, although tight junction may be opened by high osmotic pressure to efficiently increase drug permeability across blood-brain barrier (Kreuter, 2001). On the other hand, carrier-mediated systems, which may alter body drug distribution without severe intervention in the structure of tight junction, would be an excellent technique for brain-targeting delivery (Kumar, 2000). Colloidal drug carrier, one of the carrier-mediated systems, was already employed in controlled drug release with the advantages of high stability, slow drug-release rate and appropriate sustainability after administration (Govender et al., 1999; Schmidt and Bodmeier, 1999). Drugs can be incorporated with or bound to colloidal drug carriers, such as polymeric nanoparticles (NPs). For instance, azidothymidine (AZT), the first nucleoside reverse transcriptase inhibitor (NRTI) for clinical treatment of the patients infected by human immunodeficiency virus (HIV), was loaded on nanosized polyhexylcyanoacrylate (PHCA), an acrylic acid derivative, rendering an increase in its concentration in rat brains (Löbenberg et al., 1998). For in vitro tissue culture of human macrophages, which belong to cells of reticuloendothelial system, not only AZT-loaded NPs may sustain full antiviral activity (Bender et al., 1994) but also the antiviral activity of saquinavir (SQV), a protease inhibitor for the therapy of acquired immunodeficiency syndrome (AIDS), can be enhanced ten-fold by binding SQV on NPs (Bender et al., 1996).

Biocompatible polybutylcyanoacrylate (PBCA), also belonging to one of the acrylic acid derivatives, can be rapidly biodegraded and completely eliminated from body over a few days (Hillery et al., 1996). The main mechanism for PBCA degradation is the cleavage of ester side bonds and transformation of the polymers into water-soluble polymeric acids, which can be finally removed by urinary excretion. The low cytotoxicity of PBCA NPs was demonstrated by the fact that, for rat cerebrum microvascular endothelial cells, the cell viability was almost not influenced under the dosage of 10 μg/ml, and 20% reduction in the cell viability under the high dosage of 100 μg/ml was observed (Courveur et al., 1986). Hence, PBCA NPs can be a general carrier-mediated system for drug delivery. On the other hand, hydrophobicity of acrylic acid derivatives often results in less adsorption affinity to hydrophilic drugs (Hoffmann et al., 1997). Charged methylmethacrylate-sulfopropylmethacrylate (MMA-SPM) NPs may overcome this difficulty. Through application to the loading of muscarinnic agonist arecaidine propargyl ester (APE), MMA-SPM NPs were shown to be superior to other NP carriers (Langer et al., 1997b). Moreover, without any macroscopic irritation and inflammation, the administration of APE-loaded MMA-SPM NPs leaded to considerable improvement in miotic response after topical administration to the eyes of rabbits (Langer et al., 1997a). These suggest that MMA-SPM NPs can be a suitable carrier system for hydrophilic or even charged drugs.

Stavudine (D4T) is one of the most essential NTRIs for AIDS treatment with its oral bioavailability over 80%. In clinical study, D4T can appreciably increase CD4 cell counts and reduce mean serum p24 antigen levels and infectious HIV titers (Riddler et al., 1995). However, the duration of the above responses is inadequate. Furthermore, D4T is slightly hydrophilic with its $\log D_{oct} = -0.84$, where D_{oct} is the distribution coefficient between octanol and phosphate buffered saline (PBS). Thus, it is worth to investigate and compare the loading behavior of D4T on PBCA or MMA-SPM NP carriers. This is performed in the present study. Also, variation in particle diameters of the above two biodegradable NPs as a function of experimental conditions like synthesis time, stirring rate and relative content of SPM in copolymer were discussed. In particular,

the effect of lyophilization, cold storage and pH value of loading medium on the loading efficiency (LE) of D4T were investigated.

2. Materials and methods

2.1. Reagents and chemicals

The chemicals used for the synthesis of PBCA NPs include hydrochloric acid (Hayashi, Osaka, Japan), sodium hydroxide (Showa, Tokyo, Japan), dextran 70,000 (Fluka Biochemika, Buchs, Switzerland), butylcyanoacrylate (BCA, Sicomet, Sichel Werk, Hanover, Germany), and D-mannitol (Sigma, St. Louis, MO). The chemicals used for the synthesis of MMA-SPM copolymer NPs include ammonium persulfate (APS, Sigma, St. Louis, MO), methyl methacrylate (MMA, Fluka Chemica, Buchs, Switzerland), and sulfopropyl methacrylate potassium salt (SPM, Aldrich, Milwaukee, WI). Tetrahydrofuran (THF, J.T. Baker, Phillipsburg, NJ) was used for gel permeation chromatography. Ten millimolar Dulbecco's phosphate buffered saline (DPBS, Sigma, St. Louis, MO) (bisodium phosphate/monobasic potassium phosphate/sodium chloride/potassium chloride (w/w/w/w) = 1.15:0.2:8:0.2), anhydrous methanol (Mallinckrodt Baker, Phillipsburg, NJ) and acetonitrile (ACN, BDH Laboratory Supplies, Poole, England) were used for loading of D4T (Sigma, St. Louis, MO), and high performance liquid chromatography (HPLC) analysis. Ultrapure water was obtained from an Ultrapure Reverse Osmosis and Nanopure Infinity Ultrapure System (Barnstead, Dubuque, IO).

2.2. Nanoparticle preparation

PBCA NPs were synthesized by emulsion polymerization reported previously (Kreuter, 1983a) with some modifications. Briefly, an acidic polymerization medium was prepared by dissolving 0.1% (w/v) dextran 70,000 as a stabilizer in 0.01N HCl aqueous solution. 0.1% (v/v) BCA monomers were added drop by drop into the above medium under constant magnetic stirring at 750 rpm and 25 °C over 3.5 h. To complete polymerization, 0.1N NaOH was mixed with the PBCA NP suspension, which turns transiently into light blue during neutralization. For purification, the suspension was centrifuged at 5100 × *g* for 10 min. In the presence of 4% (w/v) mannitol as cryoprotectant, the milky (white) supernatant was refrigerated at −80 °C in an ultra-low temperature freezer (Sanyo, Osaka, Japan) over 30 min, and lyophilized (John Morris Scientific, Chatswood, Australia) over 24 h. The above experimental conditions for the synthesis of PBCA NPs are defined as the PBCA standard conditions except pH value of the acidic medium, which can be adjusted by HCl or NaOH.

MMA-SPM copolymer NPs were synthesized by free radical polymerization described before (Langer et al., 1996) with some modifications. Briefly, 0.05% (w/v) SPM was mixed with 4.95% (v/v) MMA in ultrapure deionized water. 0.03% (w/v) APS was added, as an initiator, into the above solution under constant magnetic stirring at 400 rpm and 78 °C over 24 h. The MMA-SPM NP suspension was filtrated through a filter paper (Toyo Roshi, Tokyo, Japan) with averaged pore size of 8 μm. After refrigeration at −80 °C over 30 min, the white filtrate in the presence of 4% (w/v) mannitol was lyophilized over 24 h. The above experimental conditions for the synthesis of MMA-SPM NPs are defined as the MMA-SPM standard conditions except the SPM percentage in total monomer, i.e., the relative content of SPM in the synthesized MMA-SPM.

In experiments for investigating the effect of lyophilization on D4T loading, NPs were not freeze-dried, and the NP suspension before lyophilization was permitted to proceed with the following characterization of particulate diameter distributions and D4T loading measurements. For these cases, the concentration of NPs in suspension was estimated by the yield of the same batch after chemical reaction, centrifugation or filtration, and free drying with mannitol.

The particle size distribution and molecular weight of the white NP powders were determined, respectively, by zeta sizer 3000 (Malvern Instruments, Worcs, UK) with photo correlation spectroscopy and gel permeation chromatography (Waters, Milford, MA) with C-18 column (Styragel, Eire, Ireland) packed with 5 μm polystyrene divinylbenzene copolymer particles. Also, the mean hydrodynamic diameters, which are sometimes called the cumulant *Z*-average diameters, of the NPs were obtained by zeta sizer 3000. The calibration curve of molecular weight for the polymers was created by polystyrene standards. The electron-microscopic images for examining the particulate diameter were

obtained by a JSM-6330 TF field emission scanning electron microscope (FE-SEM, Joel, Tokyo, Japan).

2.3. D4T loading and evaluation of loading efficiency

0.02% (w/v) D4T was dissolved in DPBS, and 0.12% (w/v) lyophilized PBCA or MMA-SPM NPs were resuspended in DPBS. An aliquot of D4T solution was mixed with an aliquot of polymer suspension. In the study of the effect of environmental pH value on D4T-loading efficiency, NaOH or HCl was first added into DPBS, whose pH value was adjusted. Thus, pH value of the D4T solution and the NP suspension were controlled. Before adjustment, pH values for D4T loading on PBCA and on MMA-SPM NPs were, respectively, 7.20 and 7.18. D4T was permitted to adsorb onto the NP surfaces under constant magnetic stirring at 150 rpm and 37 °C over 3 h to reach equilibrium loading. The D4T-loaded NPs were coated with 0.01% (relative to the total volume of the NP suspension) polysobate 80 and equilibrated in a baths-reciprocal shaker at 150 rpm and 37 °C over 30 min.

The polysobate 80-stabilized, D4T-loaded NP suspension was ultracentrifuged at $11{,}500 \times g$ for 1 h in an Eppendorf centrifuge 5415D (Eppendorf AG, Hamburg, Germany) with angle rotor. The wavelength of D4T ultraviolet absorption was determined by a UV–vis spectrophotometer (Bio-Tek Instruments, Winooski, VT) with 96-well polystyrene microplates (Nalge Nunc, Rochester, NY) and 250 nm was used as the measuring wavelength in the succeeding quantitative analysis. Unloaded (non-adsorbed) D4T content in the supernatant was assayed by high performance liquid chromatography (HPLC, Jasco, Tokyo, Japan) with reverse phase BDS Hypersil C-18 column (Thermo Hypersil-Keystone, Bellefonte, PA) packed with 5 μm particles and warmed at 60 °C by a column heater (Jones Chromatography, Walves, UK). Two high pressure HPLC pumps (PU-2080 Plus, Jasco, Tokyo, Japan) in series were employed to transport ACN gradient fluid from 5% (v/v) to 45% (v/v) over 20 min with a flow rate of 0.85 ml/min. Retention time of D4T is about 5.5–7.5 min and the detected chromatographic peaks were, then, analyzed by SISC chromatography data system. For a convenient and proper presentation of the D4T-loading data, the relative loading efficiency (LE) of D4T, based on total amount of D4T in stock solution, is defined by subtracting the residual free D4T after ultracentrifugation from the total D4T in the original loading medium, i.e.,

$$\mathrm{LE} = \frac{\text{total weight of D4T} - \text{weight of unloaded D4T}}{\text{total weight of D4T}} \times 100\%.$$

In experiments for analyzing the influence of refrigeration or cold storage on D4T loading, the polysobate 80-stablized D4T-loaded NP suspension was stocked at 4 °C over 6 weeks. Particle size distribution and LE were evaluated before and after the refrigeration treatment. The summarized procedures for the synthesis of PBCA and MMA-SPM NPs and for the D4T loading were shown in Fig. 1.

2.4. Statistical analysis

Statistical significance for the data comparison was assessed using one-way analysis of variance (ANOVA) followed by Tukey's HSD test.

3. Results and discussion

3.1. Average particle diameter (D_{av}) of NPs

Fig. 2(a) and (b) shows the typical size distributions of PBCA and MMA-SPM particles, respectively. As revealed in the figures, average particle diameter (D_{av}) of PBCA NPs is 114.2 nm and D_{av} of MMA-SPM NPs is 65.4 nm. In the following analyses, D_{av} of PBCA ranges between 100 and 300 nm and D_{av} of MMA-SPM ranges between 10 and 80 nm. In each single synthesis batch, the polydispersity index (PDI) of PBCA ranges between 0.1 and 0.3 and the PDI of MMA-SPM NPs ranges between 0.1 and 0.5, indicating narrow distributions of particle sizes of the present PBCA and MMA-SPM.

The FE-SEM images of PBCA and MMA-SPM particles are presented in Fig. 3(a)–(d). Fig. 3(a) and (b) reveals that the particulate diameters of PBCA NPs are about 150 and 200 nm, respectively. The particle diameters of MMA-SPM NPs are, respectively, about 65 and 60 nm as shown in Fig. 3(c) and (d). These results are consistent with the results obtained by the char-

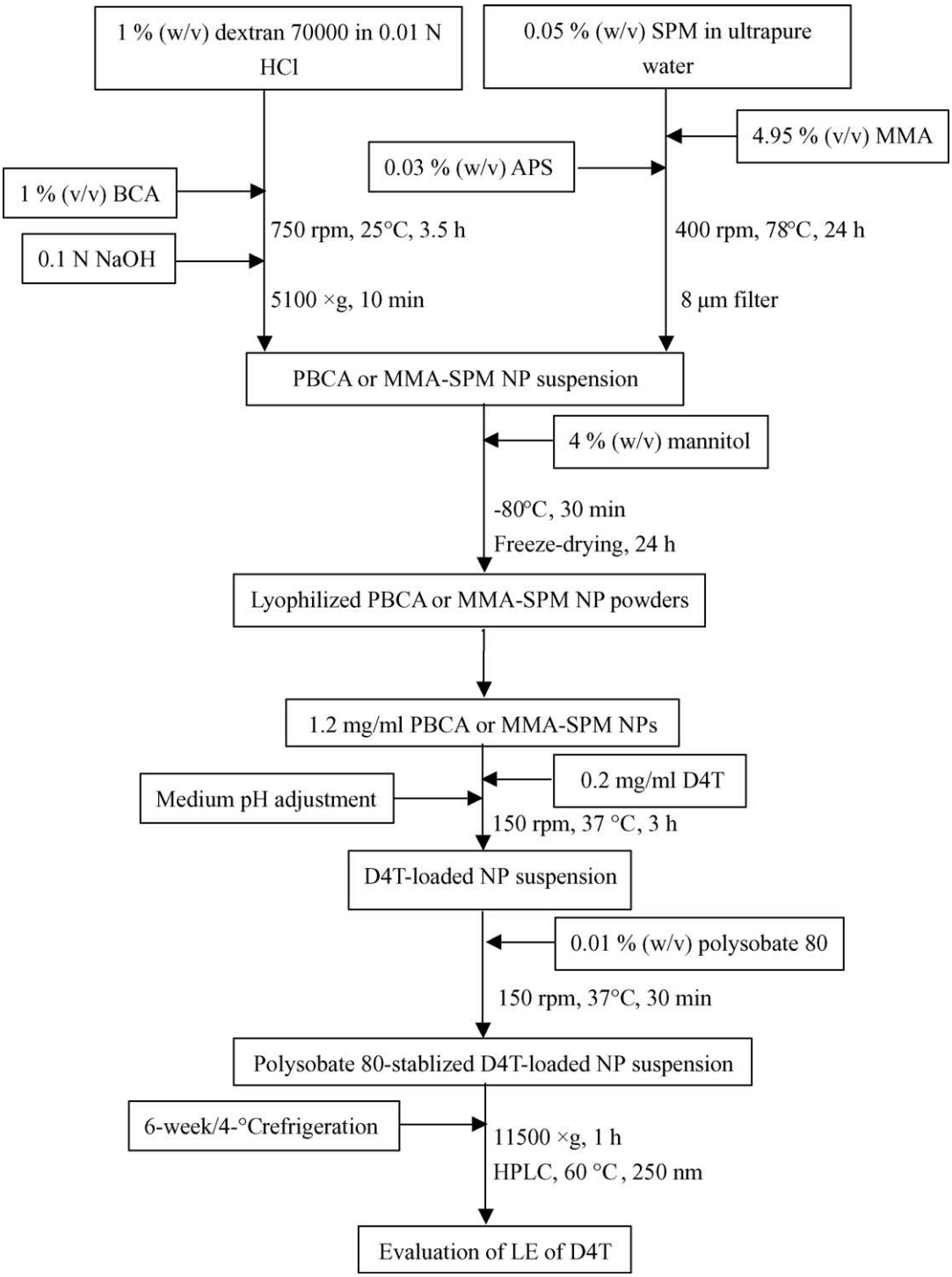

Fig. 1. Summarized procedures for the synthesis of PBCA and MMA-SPM NPs, D4T loading and LE evaluation.

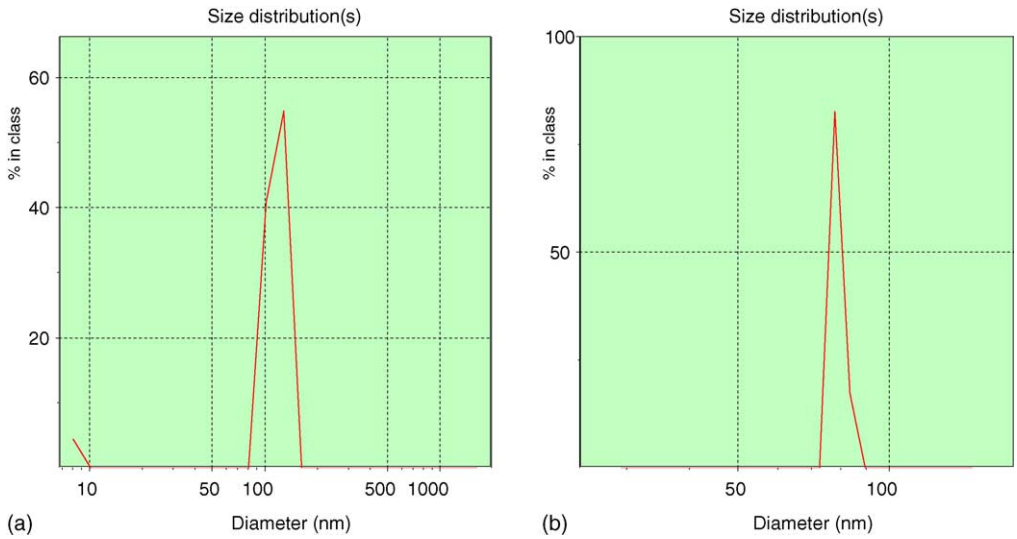

Fig. 2. Typical particle size distributions of PBCA and MMA-SPM. (a) PBCA NPs, pH 2.1, (b) MMA-SPM NPs, 1% (w/v) relative content of SPM. Key: PBCA and MMA-SPM NPs were synthesized at their standard conditions defined in the text.

acterization of zeta sizer 3000. Note that, the present PBCA and MMA-SPM NPs exhibit the morphological appearance of sphere and spheroids, respectively.

Number-averaged molecular weight (MW_{na}) of PBCA NPs and MW_{na} of MMA-SPM NPs are listed in Table 1 . Also presented in this table are the corresponding D_{av} values. The data shown in the second and third rows of Table 1 for MW_{na} of PBCA NPs, synthesized at the conditions corresponding to Fig. 3(a) and (b), are consistent with the results reported in literature that the molecular weight ranges between 20,000 and 40,000 Da for PBCA NPs with D_{av} of about 200 nm (Kreuter, 1994). MW_{na} of MMA-SPM NPs presented in the fourth and fifth rows of Table 1 imply that the present results can be comparable with the literature results where the viscosity-averaged molecular weight ranges between 35,000 and 100,000 Da for MMA-SPM NPs with D_{av} of 80–170 nm (Langer et al., 1996), although the particulate diameter and molecular weight of the present MMA-SPM NPs are obviously smaller than those of the literature. These examinations also suggest that MMA-SPM NPs are relatively smaller and denser than PBCA NPs in the present study. This is because that the charged species SPM is contained in the copolymer matrices of the former. Moreover, it can be concluded that the qualitative relation between particle size and molecular weight is that the larger D_{av}, the greater MW_{na}.

Table 1
MW_{na} and D_{av} of PBCA and MMA-SPM NPs

NP	Conditions	MW_{na} (Da)	D_{av} (nm)
PBCA	(a)	24190 ± 1705	149.2
PBCA	(b)	32239 ± 3133	202.7
MMA-SPM	(c)	27633 ± 1521	65.1
MMA-SPM	(d)	23910 ± 2532	59.5

(a), (b), (c) and (d) represent the conditions for NP synthesis, corresponding to Fig. 3(a)–(d), respectively. Statically significant difference ($p < 0.02$) between the same materials was evaluated. MW_{na} data presented here are mean ± standard deviation ($n = 3$).

For PBCA synthesis, BCA was observed to continue reacting in acidic surrounding through emulsion polymerization. Concentration of BCA monomer, kinds of acidifying agent, concentration of emulsifier, reaction temperature, stirring rate, pH value, and synthesis period can affect the resultant sizes of PBCA NPs. For monomer concentration, 2% BCA yields a minimum particle size; for acidifying agent, acetic acid leads to a much larger particle size than citric acid, sulfuric acid, nitric acid and phosphoric acid; for emulsifier concentration ranging between 0.05 and 2.5%, higher concentrations cause smaller particles; and an in-

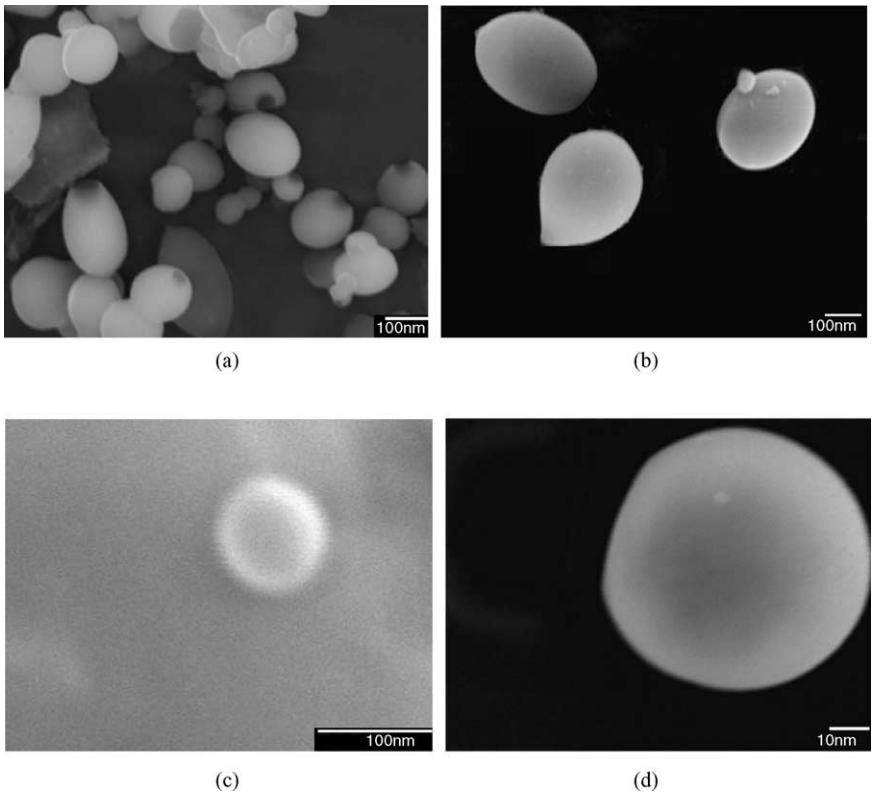

Fig. 3. FE-SEM images of PBCA and MMA-SPM particles. (a) PBCA NPs, pH 2.05, photographed under 50,000 magnification (50 k), (b) PBCA NPs, pH 5.33, photographed under 80 k, (c) MMA-SPM NPs, 1% (w/v) relative content of SPM, photographed under 100 k, and (d) MMA-SPM NPs, 5% (w/v) relative content of SPM, photographed under 100 k. Key: same as Fig. 2.

crease in reaction temperature ranging between 4 and 80 °C seems to has obscure effect on particle size with an increase of PDI (Douglas et al., 1984).

Fig. 4 shows the variation in D_{av} of PBCA NPs, synthesized at pH 1.5 and the PBCA standard conditions except synthesis time, t, and stirring rate, w, as a function of t. For the case of 750 rpm, t ranging between 3.5 and 7 h does not strongly influence D_{av}, which ranges between 220 and 230 nm, as revealed in Fig. 4. As also presented in this figure, D_{av} increases dramatically with t, which ranges between 7 and 10.5 h, for 750 rpm. This is because that a long period for synthesis of PBCA beads can increase the possibility of linkage among a number of large particles, which exist in the suspension for about 7 h of polymerization, rendering a large D_{av}. In this case, 7 h is defined as the characteristic time for dramatic increase in particle size, t_c. For the 500 rpm case exhibited in Fig. 4, D_{av} steadily increases from about 190 to 220 nm when t increases from 3.5 to 9 h, and D_{av} appreciably increases when t is longer than 9 h ($t_c = 9$ h). The rationale behind this result is the same as that for the case of 750 rpm. The above results also suggest that the time required for significant increase in D_{av} becomes longer for a lower w. Furthermore, it can generally be drawn that a longer t or a higher w can cause larger particles. A high w yields a large shear stress, which may break the newly synthesized NPs into fractures. On the other hand, a high w also yields high kinetic energy of NPs, which renders the oligomers, semisolids and large particles to overcome the interfacial energy barriers, forming resultant particles with large D_{av}. In the present study, the effect of particulate kinetic energy is greater than that of fluidic shear stress. Additionally, when t is less than 1.5 h, distribution of particle sizes with almost independent two

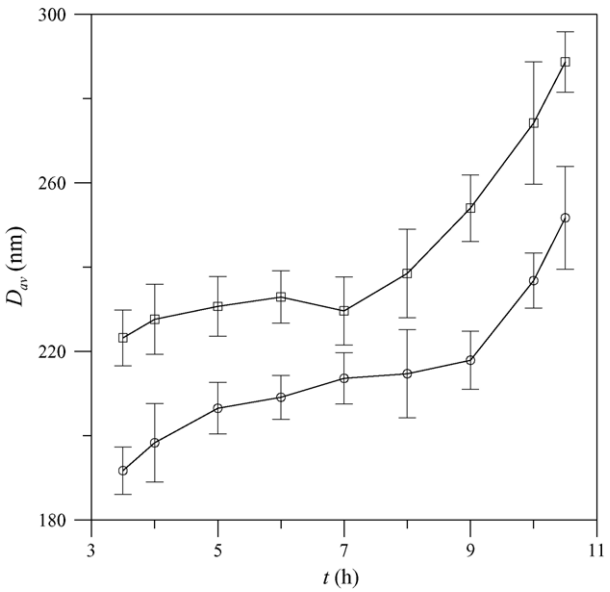

Fig. 4. Variation in D_{av} of PBCA NPs as a function of t for the case of pH 1.5. (□) 750 rpm; (◯) 500 rpm. Key: 1% (w/v) BCA, 1% dextran and 25 °C. For fixed t, statically significant difference ($p < 0.05$) between samples of different w was evaluated. Data presented here are mean ± standard deviation ($n = 3$).

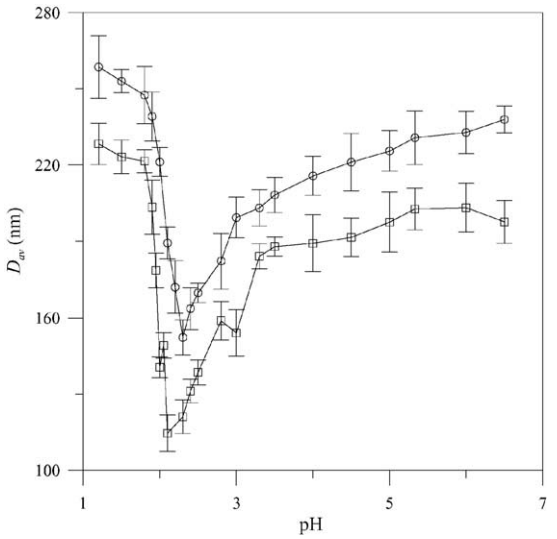

Fig. 5. Variation in D_{av} of PBCA NPs as a function of medium pH value. (□) 3.5 h; (◯) 9 h. Key: same as Fig. 4 and 750 rpm. For fixed medium pH value, statically significant difference ($p < 0.02$) between samples of different t was evaluated. Data presented here are mean ± standard deviation ($n = 3$).

peaks was obtained, indicating that covalent linkage and/or agglomeration between the two particle groups are at nonequilibrium state.

Variation in D_{av} of PBCA NPs synthesized at the PBCA standard conditions, except medium pH value and t, as a function of medium pH value is presented in Fig. 5. As shown in this figure, an increase in pH from 1.2 to 1.8 leads to a smooth decrease in D_{av} from about 230 to 220 nm, for the case of $t = 3.5$ h. An increase in pH from 1.8 to 2.1, for the case of $t = 3.5$ h, leads to a drastic decrease in D_{av}, and D_{av} increases radically with pH from 2.1 to 3.5. Further increases in pH until pH 6.5 yield D_{av} ranging between 185 and 205 nm for the case of $t = 3.5$ h, as exhibited in Fig. 5. As also presented in this figure, the relation between D_{av} and pH value for the case of $t = 9$ h is similar to that of $t = 3.5$ h. It can be found that the minimum D_{av} is reached at pH 2.1 and 2.3 for the case of $t = 3.5$ and 9 h, respectively, indicating that pH value for the minimum D_{av}, pH_m, can be slightly shifted to a higher pH value by a longer t. This observation may be in agreement with literature where the minimum D_{av} locates at pH 2.0 although the literature data presented PBCA NPs with D_{av} between 200 and 300 nm (Kreuter, 1994). Note that D_{av} varies from 110 to 260 nm in the present study. Steadily increase in D_{av} from about 200 to 240 nm is obtained as pH value increases from 3 to 6.5 for the case of $t = 9$ h. In the pH range from 1.2 to 6.5, D_{av} for the case of $t = 9$ h is larger than that of $t = 3.5$ h. This is consistent with the result exhibited in Fig. 4. Additionally, it can be also concluded that D_{av} at pH lower than 1.8 (low pH) is larger than D_{av} at pH higher than 3.5 (high pH) for both cases of $t = 3.5$ and 9 h.

In the process of free-radical polymerization of MMA-SPM, SPM monomer content, total monomer percentage, and stirring rate may play influential roles in the outcome of MMA-SPM NP diameters. For SPM concentration, the particulate diameter decreases with an increase in SPM content from 0 to 10%, and further increase in SPM concentration until 50% has nearly no effect on the size of MMA-SPM NPs; a high total monomer percentage yields a large particle size; and ASP concentration, ranging between 0.01 and 0.3%, has no obvious effect on particle sizes, and low reproducibility was found when ASP concentration is 0.5% (Langer et al., 1996).

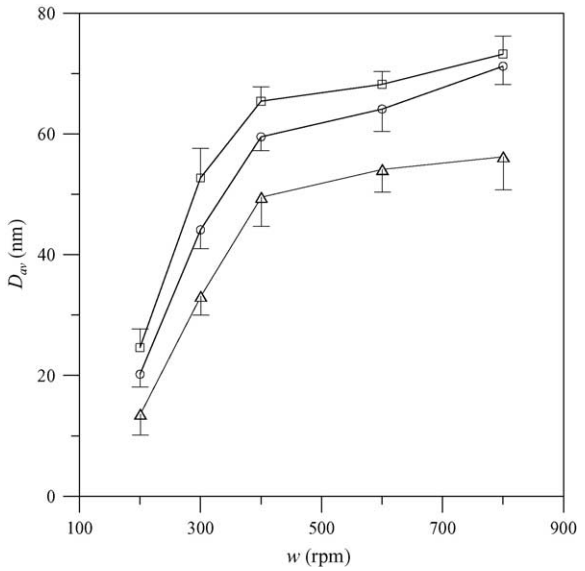

Fig. 6. Variation in D_{av} of MMA-SPM NPs as a function of w. Relative content of SPM: (□) 1% (w/v); (◯) 5% (w/v); (△) 9% (w/v). MMA-SPM NPs were synthesized at the MMA-SPM standard conditions, except stirring rate. For fixed w, statically significant differences ($p < 0.05$) among samples of different relative content of SPM were evaluated. Data presented here are mean ± standard deviation ($n = 3$).

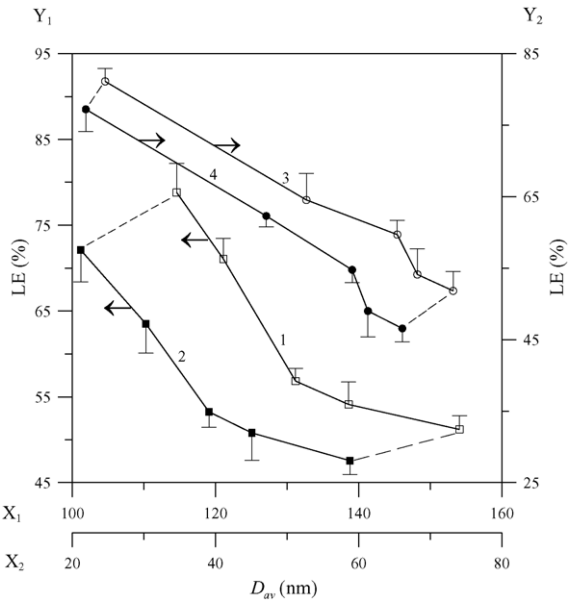

Fig. 7. Variation in LE of D4T as a function of D_{av}. (□) PBCA NPs with lyophilization; (■) PBCA NPs without lyophilization; (◯) MMA-SPM NPs with lyophilization; (●) MMA-SPM NPs without lyophilization. Five corresponding pairs, with and without lyophilization, of PBCA NPs and of MMA-SPM NPs are connected by the dash lines. The axes for broken line 1 and 2 (PBCA NPs) are X_1–Y_1, and broken lines 3 and 4 (MMA-SPM NPs) use X_2–Y_2. Statically significant difference ($p < 0.05$) between the same NP with and without lyophilization was evaluated. Data presented here are mean ± standard deviation ($n = 3$).

Variation in D_{av} of MMA-SPM NPs as a function of w is shown in Fig. 6. As revealed in this figure, D_{av} ranges approximately between 10 and 80 nm, indicating rather small particles relative to PBCA NPs. For a fixed relative content of SPM in copolymer, the higher w, the larger the polymeric particles. The reason behind this fact is the effect of kinetic energy, discussed in the previous paragraph for Fig. 4. For a fixed w, the higher the relative content of SPM in copolymer, the smaller D_{av}. This qualitative trend is consistent with previous observations, although the present MMA-SPM NPs are apparently smaller than those of literature (Langer et al., 1996). Since SPM is negatively charged, the monomers repel each other in the reaction medium via electrostatic interactions. Thus, the probability of collision among SPM molecules or SPM-incorporated oligomers is reduced. Besides, higher SPM percentage in MMA-SPM copolymer causes a stronger electrostatic effect among the newly formed polymers, rendering a larger electrical double-layer repulsion resulted from the nearby electrolyte fluids around the NPs (Kuo, 2003b). This prevents the charged tiny particle from incessant polymerization or aggregation to become a large particle (Kuo, 2003a).

Fig. 7 presents the variation in LE of D4T as a function of D_{av}. PBCA NPs applied in the present D4T loading study are manufactured at various medium pH values and the PBCA standard conditions, except lyophilization process. MMA-SPM NPs used in this D4T loading are synthesized at various w values, 1% (w/v) relative content of SPM and the MMA-SPM standard conditions, except w and lyophilization process. Solid data denote the results without lyophilization process. Physical adsorption and ionic interaction may be, respectively, the main contribution to the loading of hydrophilic D4T on neutral PBCA surfaces and on negatively charged MMA-SPM surfaces. Since the specific surface area for D4T loading of small particles is normally higher than that of large particles, the larger D_{av},

the lower LE, as indicated in Fig. 7. Comparing lines 1 with 2, and lines 3 with 4 in Fig. 7, D_{av} becomes larger with lyophilization for both of the two kinds of polymeric NPs. Moreover, LE of D4T on each specific kind of the two NPs becomes higher with lyophilization, in general, as exhibited in Fig. 7. Although the above statement about the relation between specific surface area for D4T loading and particle size is generally correct, lyophilization yields larger particles and higher LEs for PBCA NPs and MMA-SPM NPs. This result suggests that the lyophilization process can increase the size of NPs and their D4T loading ability through flocculation during freeze drying and/or effect of mannitol added as a cryoprotectant. PBCA NPs were found to agglomerate after lyophilization (Kreuter, 1983b; Sommerfeld et al., 1997). For oligonucleotide-entrapped poly (D,L-lactic acid) NPs, a slight increase in mean size were obtained after freeze drying (Berton et al., 1999). In a study of Dynasan- or Compritol-incorporated solid lipid nanoparticles (Schwarz and Mehnert, 1997), behavior of cryoprotectants was regarded as the key factor in maintaining particulate size. Note that NPs employed in the lines 1 and 3 of Fig. 7 were lyophilized with the existence of mannitol. The same batch of PBCA NPs lyophilized with and without mannitol yields, respectively, D_{av} = 122.7 and 208.1 nm; and the same batch of MMA-SPM NPs lyophilized with and without mannitol yields, respectively, D_{av} = 64.2 and 119.3 nm. This indicates that mannitol adequately plays a role of a cryoprotectant in separating NPs from one another, maintaining high dispersity of NPs, and preventing NPs from aggregation.

Variation in LE of D4T as a function of D_{av} is also exhibited in Fig. 8. PBCA NPs used in this D4T loading are synthesized at pH 2.4 and the PBCA standard conditions, except t = 3.5, 7 and 9 h. MMA-SPM NPs used in the present D4T loading research are prepared at the MMA-SPM standard conditions and the relative content of SPM = 1, 5 and 9% (w/v). Solid data represent the results after 6-week/4 °C refrigeration. Comparing lines 1 with 2, and lines 3 with 4 in Fig. 8, cold storage yields an increase in D_{av} and a decrease in LE of D4T for the two kinds of D4T-loaded NPs. Influence of cold storage on the increase in D_{av} of PBCA NP suspension is stronger than that of MMA-SPM NP suspension, as presented in Fig. 8. Interestingly, storage at 25 or 42 °C yields poor stability of PBCA NPs (Sommerfeld et al., 1997). Fig. 8 also reveals that the effect of cold storage on the decrease in LE of D4T for PBCA NPs is more sensitive than that for MMA-SPM NPs, indicating that D4T-loaded MMA-SPM NP suspension would be more suitable for cold storage than PBCA NP suspension. Although after the refrigeration treatment, the desorption of D4T from PBCA NPs is greater than that from MMA-SPM NPs, the decreases in LE of D4T on PBCA NPs and on MMA-SPM NPs are all less than 6 and 3%, respectively. These results demonstrate that the stability of D4T on the two kinds of the biocompatible NPs is high. For D4T-loaded MMA-SPM NPs, LE of D4T increases with the relative content of SPM, as suggested in Fig. 8. This is because that a higher relative content of SPM leads to not only smaller but also higher negatively charged NPs. Smaller carriers possess larger specific surface area for D4T loading, and higher charged carriers display stronger affinity

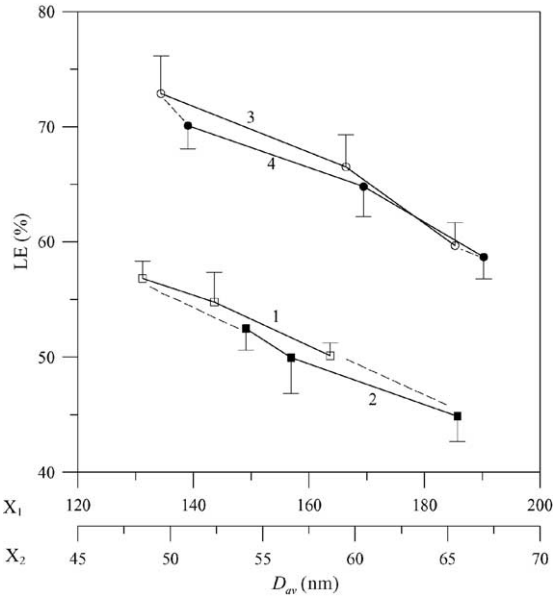

Fig. 8. Variation in LE of D4T as a function of D_{av}. (□) PBCA NPs without 6-week/4 °C refrigeration; (■) PBCA NPs with 6-week/4 °C refrigeration; (○) MMA-SPM NPs without 6-week/4 °C refrigeration; (●) MMA-SPM NPs with 6-week/4 °C refrigeration. Three corresponding pairs, with and without 6-week/4 °C refrigeration, of PBCA NPs and of MMA-SPM NPs are connected by the dash lines. X_1 and X_2 axes are employed, respectively, for the broken lines 1 and 2 (PBCA NPs), and the broken lines 3 and 4 (MMA-SPM NPs). Statically significant difference ($p < 0.05$) between the same NP with and without 6-week/4 °C refrigeration was evaluated. Data presented here are mean ± standard deviation (n = 3).

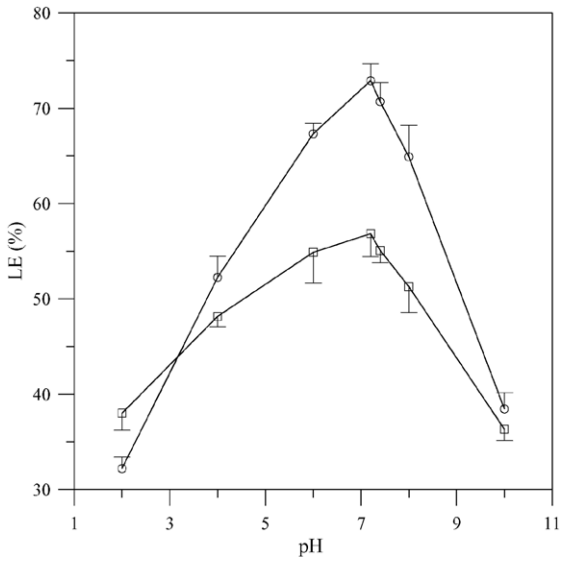

Fig. 9. Variation in LE of D4T as a function of pH value of D4T loading medium. (□) PBCA NPs, pH 2.4; (◯) MMA-SPM NPs, 9% (w/v) relative content of SPM. PBCA and MMA-SPM NPs were synthesized at their standard conditions defined in the text. For fixed pH value of D4T loading medium, statically significant difference ($p < 0.05$) between samples of PBCA NPs and MMA-SPM NPs was evaluated. Data presented here are mean ± standard deviation ($n = 3$).

to hydrophilic D4T, rendering larger amount of D4T adsorption on the particle surfaces. For D4T-loaded PBCA NPs, a higher LE of D4T can be obtained by smaller particles (shorter t), as implied in Fig. 8. In the D_{av} range shown in Fig. 8, LE of D4T on MMA-SPM NP surfaces is higher than that on PBCA NP surfaces, in general.

For anti-HIV treatment, especially for oral administration, surrounding pH value for D4T absorption and metabolism may vary severely. Since variation in pH value in gastrointestinal tract is serious, it seems to be a necessity to study the influence of pH value of loading environment on LE of D4T. Fig. 9 shows the variation in LE of D4T as a function of pH value of D4T loading medium. As indicated in Fig. 9, maximum LE of D4T on each of the two NPs is achieved at the original pH value before adjustment, i.e., pH 7.2. Any adjustment (increase or decrease) in medium pH value reduces LE of D4T. The main reason for the result is that excess ions involved via pH adjustment in the loading medium may be adsorbed onto NP surfaces, rendering occupation of loading sites and desorption of D4T. Otherwise, interaction between excess ions and D4T in medium may hinder D4T from loading onto particulate surfaces. Drugs are considered to be loaded on NP surfaces by physical adsorption, and variation in environmental pH value from philological value may simply lead to desorption of drugs (Hillery et al., 1996). As revealed in Fig. 9, the effect of reduction in LE of D4T by pH variation for MMA-SPM NPs is larger than that for PBCA NPs, indicating LE of D4T on MMA-SPM NPs is more sensitive to pH variation than that on PBCA NPs. This is because that the competition between excess cations (or protons) and D4T molecules for the effective adsorption sites on negatively charged MMA-SPM NPs is keener than that on PBCA NPs. Note that at pH 7.4, LE of D4T on MMA-SPM NPs is larger than that on PBCA NPs. Thus, we conclude that PBCA NPs are superior to MMA-SPM NPs for oral D4T administration, and for intravenous D4T treatment, MMA-SPM NPs can be better than PBCA NPs.

4. Conclusions

In summary, application of PBCA and MMA-SPM NPs to the loading of D4T was presented. Here, the biodegradable PBCA NPs and MMA-SPM copolymer NPs were synthesized, respectively, by emulsion polymerization and free radical polymerization. The results reveal that the longer the synthesis time (t) and the higher the stirring rate (w), the larger the PBCA average particle diameter (D_{av}). High w also yields short characteristic t for dramatic increase in PBCA particle size. In the present study, the range of medium pH value for minimum D_{av}, pH_m, for PBCA NPs is between 2.1 and 2.3 and pH_m increases with t. For MMA-SPM NPs, the higher w and the lower the relative content of SPM in copolymer, the larger D_{av}. For both of the two kinds of NPs, the larger D_{av}, the smaller LE of D4T. Lyophilization process or cold storage at 4 °C over 6 weeks causes an increase in D_{av} for both of the two kinds of NPs. Moreover, lyophilization process increases LE of D4T, in general; cold storage, however, slightly decreases LE of D4T. Variation in pH value of D4T loading medium from pH 7.2 leads to a reduction in LE of D4T for the two NPs. Additionally, MMA-SPM NPs are less stable than PBCA NPs when pH value of D4T loading medium varies from pH 7.2. However, at physiological pH value, LE of D4T on MMA-SPM NPs is larger

than that on PBCA NPs. The present loaded NPs can readily be applied to the transport of anti-HIV drug through brain microvascular endothelial cells to evaluate the possibly promoted permeability across blood-brain barrier.

Acknowledgment

This work is supported by the National Science Council of the Republic of China.

References

Bender, A., von Briesen, H., Kreuter, J., Ducan, I.B., Rubsamen-Waigmann, H., 1996. Efficiency of nanoparticles as carrier system for antiviral agents in human immunodeficiency virus-infected human monocytes/macrophages in vitro. Antimicrob. Agents Chemother. 40, 1467–1471.

Bender, A., Schafer, V., Steffan, A., Royer, C., Kreuter, J., Rubsamen-Waigmann, H., von Briesen, H., 1994. Inhibition of HIV in vitro by antiviral drug-targeting using nanoparticles. Res. Virol. 145, 215–220.

Berton, M., Allemann, E., Stein, C.A., Gurny, R., 1999. Highly loaded nanoparticulate carrier using a hydrophobic antisense oligonucleotide complex. Eur. J. Pharm. Sci. 9, 163–170.

Courveur, P., Grislain, L., Lenaerts, V., Brasseur, F., Guiot, P., Biernacki, A., 1986. Biodegradable polymeric nanoparticles as drug carrier for antitumor agents. In: Guiot, P., Courveur, P. (Eds.), Polymeric Nanoparticles and Microshpheres. CRC Press, Boca Raton, FL, pp. 27–93.

Douglas, S.J., Illum, L., Davis, S.S., Kreuter, J., 1984. Particles size and size distribution of poly(butyl-2-cyanoacrylate) nanoparticles. I. Influence of physicochemical factors. J. Colloid Interface Sci. 101, 149–158.

Govender, T., Stolnik, S., Garnett, M.C., Illum, L., Davis, S.S., 1999. PLGA nanoparticles prepared by nanoprecipitation: drug loading and release studies of a water soluble drug. J. Control. Release 57, 171–185.

Hillery, A.M., Toth, I., Shaw, A.J., Florence, A.T., 1996. Copolymerised peptide particles (CPP). I: Synthesis, characterization and in vitro studies on a novel oral nanoparticulate delivery system. J. Control. Release 41, 271–281.

Hoffmann, F., Cinatl Jr., J., Kabicková, H., Cinatl, J., Kreuter, J., Stieneker, F., 1997. Preparation, characterization and cytotoxicity of methylmethacrylate copolymer nanoparticles with a permanent positive surface charge. Int. J. Pharm. 157, 189–198.

Kreuter, J., 2001. Nanoparticulate systems for brain delivery of drugs. Adv. Drug Deliv. Rev. 47, 65–81.

Kreuter, J., 1994. Nanoparticles. In: Kreuter, J. (Ed.), Colloidal Drug Delivery Systems. Mercel Dekker, New York, pp. 219–342.

Kreuter, J., 1983a. Evaluation of nanoparticles as drug delivery systems. I. Preparation methods. Pharm. Acta Helv. 58, 196–209.

Kreuter, J., 1983b. Physicochemical characterization pf polyacrylic nanoparticles. Int. J. Pharm. 14, 43–58.

Kumar, M.N.V.R., 2000. Nano and microparticles as controlled drug delivery devices. J. Pharm. Pharmaceut. Sci. 3, 234–258.

Kuo, Y.C., 2003a. Effects of sizes of charged species on the flocculation of biocolloids: absorption of cations in membrane layer. J. Chem. Phys. 118, 398–406.

Kuo, Y.C., 2003b. Effects of particulate curvature and sizes of charged species on the adsorption of a biocolloid bearing nonuniformly distributed fixed charges. J. Chem. Phys. 118, 8023–8032.

Langer, K., Mutschler, E., Lambrecht, G., Mayer, D., Troschau, G., Stieneker, F., Kreuter, J., 1997a. Methylmethacrylate sulfopropylmethacrylate copolymer nanoparticles for drug delivery. Part III: Evaluation as drug delivery system for ophthalmic applications. Int. J. Pharm. 158, 219–231.

Langer, K., Stieneker, F., Lambrecht, G., Mutschler, E., Kreuter, J., 1997b. Methylmethacrylate sulfopropylmethacrylate copolymer nanoparticles for drug delivery. Part II: Arecaidine propargyl ester and pilocarpine loading and in vitro release. Int. J. Pharm. 158, 211–217.

Langer, K., Marburger, C., Berthold, A., Kreuter, J., Stieneker, F., 1996. Methylmethacrylate sulfopropylmethacrylate copolymer nanoparticles for drug delivery. Part I: Preparation and physiochemical characterization. Int. J. Pharm. 137, 67–74.

Löbenberg, R., Araujo, L., von Briesen, H., Rodgers, E., Kreuter, J., 1998. Body distribution of azidothymidine bound to hexylcyanoacrylate nanoparticles after i.v. injection to rats. J. Control. Release 50, 21–30.

Riddler, S.A., Anderson, R.E., Mellors, J.W., 1995. Antiretrovial activity of stavudine (2′,3′-didehydro-3′-deoxythymidine, D4T). Antiretrovial Res. 27, 189–203.

Schmidt, C., Bodmeier, R., 1999. Incorporation of polymeric nanoparticles into solid dosage forms. J. Control. Release 57, 115–125.

Schwarz, C., Mehnert, W., 1997. Freeze-drying of drug-free and drug-loaded solid lipid nanoparticles (SLN). Int. J. Pharm. 157, 171–179.

Sommerfeld, P., Schroeder, U., Sabel, B.A., 1997. Int. J. Pharm. 155, 201–207.